Meteoritics & Planetary Science 39, Nr 9, 1495–1508 (2004)
Abstract available online at http://meteoritics.org

Shocked rocks and impact glasses from the El'gygytgyn impact structure, Russia

Eugene P. GUROV[1] and Christian KOEBERL[2*]

[1]Institute of Geological Sciences, National Academy of Sciences of the Ukraine, 55b Oles Gontchar Street, Kiev 01054, Ukraine
[2]Department of Geological Sciences, University of Vienna, Althanstrasse 14, A-1090 Vienna, Austria
*Corresponding author. E-mail: christian.koeberl@univie.ac.at

(Received 18 July 2003; revision accepted 4 May 2004)

Abstract–The El'gygytgyn impact structure is about 18 km in diameter and is located in the central part of Chukotka, arctic Russia. The crater was formed in volcanic rock strata of Cretaceous age, which include lava and tuffs of rhyolites, dacites, and andesites. A mid-Pliocene age of the crater was previously determined by fission track (3.45 ± 0.15 Ma) and $^{40}Ar/^{39}Ar$ dating (3.58 ± 0.04 Ma). The ejecta layer around the crater is completely eroded. Shock-metamorphosed volcanic rocks, impact melt rocks, and bomb-shaped impact glasses occur in lacustrine terraces but have been redeposited after the impact event.

Clasts of volcanic rocks, which range in composition from rhyolite to dacite, represent all stages of shock metamorphism, including selective melting and formation of homogeneous impact melt. Four stages of shocked volcanic rocks were identified: stage I (≤35 GPa; lava and tuff contain weakly to strongly shocked quartz and feldspar clasts with abundant PFs and PDFs; coesite and stishovite occur as well), stage II (35–45 GPa; quartz and feldspar are converted to diaplectic glass; coesite but no stishovite), stage III (45–55 GPa; partly melted volcanic rocks; common diaplectic quartz glass; feldspar is melted), and stage IV (>55 GPa; melt rocks and glasses). Two main types of impact melt rocks occur in the crater: 1) impact melt rocks and impact melt breccias (containing abundant fragments of shocked volcanic rocks) that were probably derived from (now eroded) impact melt flows on the crater walls, and 2) aerodynamically shaped impact melt glass "bombs" composed of homogeneous glass. The composition of the glasses is almost identical to that of rhyolites from the uppermost part of the target. Cobalt, Ni, and Ir abundances in the impact glasses and melt rocks are not or only slightly enriched compared to the volcanic target rocks; only the Cr abundances show a distinct enrichment, which points toward an achondritic projectile. However, the present data do not allow one to unambiguously identify a meteoritic component in the El'gygytgyn impact melt rocks.

INTRODUCTION

The El'gygytgyn impact crater is situated in the central mountainous area of the Chukotka Peninsula, Russia, centered at 67°30′N and 172°34′E (Fig. 1). The El'gygytgyn depression was discovered in 1933 from an aerogeological study of this region (Obruchev 1957); in comparison with lunar craters, this author suggested a volcanic origin for El'gygytgyn. The possible impact origin of the crater was first proposed by Nekrasov and Raudonis (1963). However, because these authors did not find coesite in eight thin sections of volcanic rocks from the crater rim, they concluded that the structure has a tectonic origin. Nevertheless, Zotkin and Tsvetkov (1970) and Engelhardt (1974) included the El'gygytgyn depression in their lists of probable impact structures. Using these data, Dietz and McHone (1976) studied LANDSAT images of the site and concluded that it is probably the largest Quaternary impact crater on Earth. Shortly thereafter, Dietz (1977) suggested that the El'gygytgyn crater could be a possible source of the Australasian tektites.

The impact origin of the El'gygytgyn structure was confirmed by Gurov and co-authors from the recognition of shock metamorphic effects in the volcanic rocks from the crater (Gurov et al. 1978, 1979a, b). Subsequent petrological, geochemical, and geophysical studies of the El'gygytgyn impact crater and its rocks have been carried out by Feldman et al. (1981), Dabija and Feldman (1982), and Kapustkina et al. (1985).

The age of the El'gygytgyn impact crater was determined

© Meteoritical Society, 2004. Printed in USA.

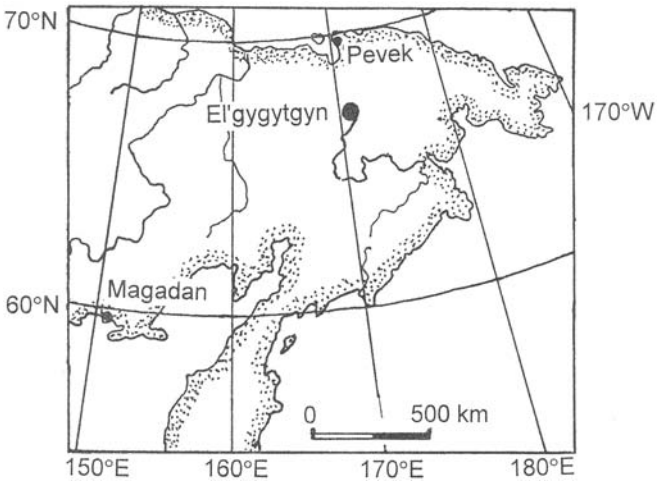


Fig. 1. Location of the El'gygytgyn impact crater on the Chukotka Peninsula, northeast Russia.

to be 4.52 ± 0.11 Ma by fission track dating (Storzer and Wagner 1979), 3.45 ± 0.15 Ma by later fission track dating (Komarov et al. 1983), and 3.50 ± 0.50 Ma by K-Ar dating (Gurov et al. 1979b). The most recent $^{40}Ar/^{39}Ar$ date yielded an age of the impact glasses of 3.58 ± 0.04 Ma (Layer 2000), which is in good agreement with the earlier data. All these dates exclude a relation between the Australasian tektites and the El'gygytgyn crater.

During the last years, the El'gygytgyn crater and, especially, its post-impact sedimentary record have been intensely investigated in a joint program of the Alfred-Wegener Institute, Potsdam, Germany, the University of Massachusetts, Amherst, USA, and the North-East Interdisciplinary Scientific Research Institute, Magadan, Russia. A 12.7 m-long core of the lake sediments was studied for paleoclimatic information of this continental region of the Arctic (Brigham-Grette et al. 1998; Nowaczyk et al. 2002). The dynamics and morphology of ice covering the El'gygytgyn Lake were studied from radar satellite data by Nolan et al. (2003), who also speculated on the location of a possible central uplift that is buried by the lake sediments.

The purpose of the present paper is to summarize for the international literature some geological and petrographic observations on the El'gygytgyn structure made by one of us (E. Gurov) over several decades, supplemented by some new petrographic and geochemical data.

GEOLOGIC BACKGROUND

The El'gygytgyn crater is a flat-floored circular basin with a rim-rim diameter of about 18 km (Fig. 2) that is situated in the central part and southeastern slope of the Academician Obruchev Ridge in central Chukotka. The crater floor, about 14 km in diameter, is occupied by the nearly circular El'gygytgyn Lake, which is 12 km in diameter and up to 170 m deep in its center. A complex system of lacustrine

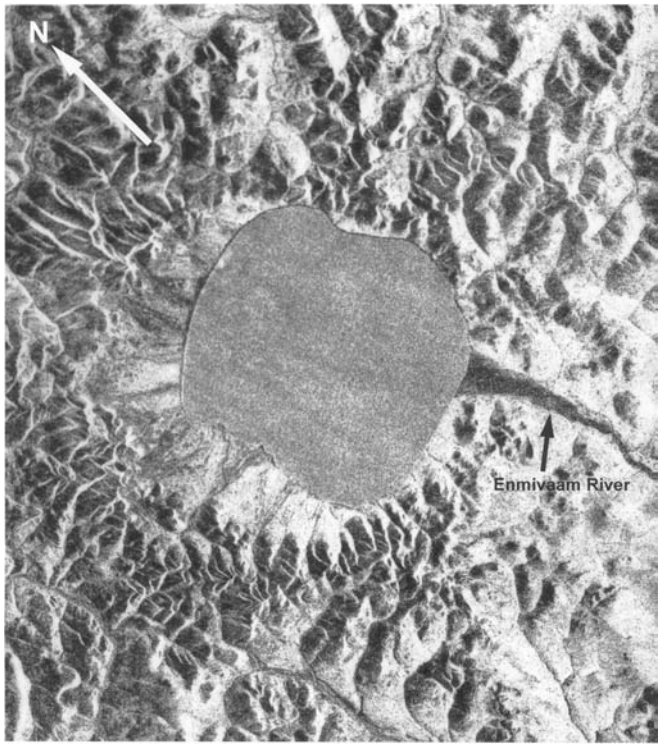


Fig. 2. Satellite (Seasat SAR) image of the El'gygytgyn impact crater. The crater floor is occupied by the El'gygytgyn Lake, about 12 km in diameter. The Enmivaam River (dark in the image, marked with arrow) crosses the crater rim in its southeastern part. North is shown with an arrow. Image courtesy J. Garvin (NASA Goddard Space Flight Center).

terraces surrounds the lake. The highest terrace is about 80 m above the lake level, and the lowest one is 1–3 m high. Thirty-eight streams run into the lake, and only the Enmivaam River flows out of the lake and determines the water level in it. A central peak is not exposed on the recent surface of the crater floor. Gravity measurements by Dabidja and Feldman (1982) indicate the presence of a central peak, about 2 km in diameter, underneath post-impact sediments, centered relative to the crater outline. In contrast, Nolan et al. (2003) suggest from radar images that the central uplift might be centered relative to the lake outline (i.e., asymmetric relative to the actual crater). New seismic data (F. Niessen, personal communication to C. Koeberl 2004) seem to agree better with the earlier gravity data.

The crater is surrounded by an uplifted rim that has an asymmetrical cross section, with steep inner walls and gentle outer slopes. The average height of the rim, about 180 m above the lake level and 140 m above the surrounding area, was calculated from 24 radial morphological profiles of the crater. The initial height of the rim before erosion was estimated to be about 230 m (Gurov and Yamnichenko 1995). A low concentric outer rim was discovered by morphological investigations of the structure. The height of the second rim is up to 14 m at a distance of 1.75 crater radii.

A complex system of faults surrounds the crater (Fig. 3). Short radial faults predominate, while concentric arcuate faults and some other fault types are subordinate around the impact structure. The lengths of the faults range from 0.5 km to 10 km. In some cases, they are expressed on the surface as trenches that are one to several m wide. Fault zones are composed of poorly consolidated detrital material with fine-grained matrix without any indications of hydrothermal alteration.

The areal distribution of faults around the El'gygytgyn crater was studied using aerial photographs. The highest fault density occurs within the inner walls of the structure at a distance of 0.9–1.0 crater radii from the center. The areal density of the fault system decreases outward from the crater rim to a distance of about 2.7 crater radii, where it reaches the regional level (Gurov and Gurova 1983).

Megablock breccia zones occur at the northern and western inner slopes of the crater rim within an area of about 4 km^2. The megabreccia shows a gradual transition to intensely faulted crater rim and is buried underneath lacustrine sediments. Block sizes in the megabreccia range from tens to hundreds of m. They are cemented by detrital material. These blocks are poorly exposed in relief but are visible in aerial photographs. The blocks of the megabreccia are composed of rhyolites, ignimbrites, and rhyolite tuffs. No shock metamorphic effects have been noted in the rocks of the crater rim.

The target rocks of the crater comprise the volcanic strata of the Pykarvaam and Milguveem series of Albian to Cenomanian age (Kotlar et al. 1981; Feldman et al. 1981). Laser $^{40}Ar/^{39}Ar$ dating of the volcanic rocks of the crater basement show ages from 83.2 to 89.3 Ma (Layer 2000). The volcanic rocks include lava, tuffs, and ignimbrites of rhyolites and dacites, rarely andesites and andesitic tuffs (Fig. 4). These deposits dip gently with 6° to 10° to the east-southeast. A generalized sequence of the strata was composed using the separate sections of the volcanic rock complex exposed at the crater and partly on the outer slopes of the rim (Gurov and Gurova 1991). From top to bottom, the exposed rocks are: ignimbrites (250 m), tuffs and lava of rhyolites (200 m), tuffs and lava of andesites (70 m), ash tuffs and welded tuffs of rhyolites and dacites (≥100 m).

Thus, the thickness of the whole exposed section is more than 600 m. This section of volcanic rock strata corresponds to the western, northern, and northeastern sections of the crater area, while dacite and andesite lava and tuff predominate in its southeastern part. A basalt plateau, about 0.75 km^2 in size and 110 m thick, occurs on the surface of the rhyolites and ignimbrites in the northeastern part of the crater rim, but shocked basalts are very rare in the crater. The composition of the main types of volcanic rocks of the crater basement is presented in Table l. The average target rock composition given in Table 1 was calculated from the relative thicknesses of the target rocks described in the previous paragraph.

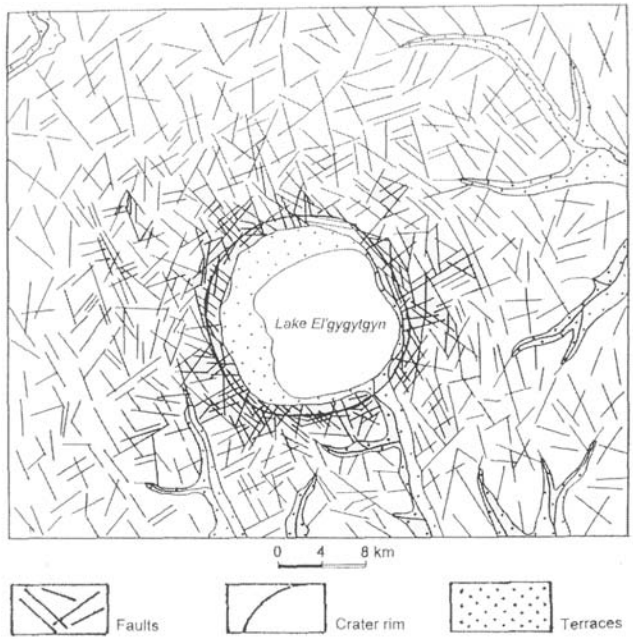


Fig. 3. Fault system around the El'gygytgyn impact crater (after field work by E. Gurov and E. Gurova).

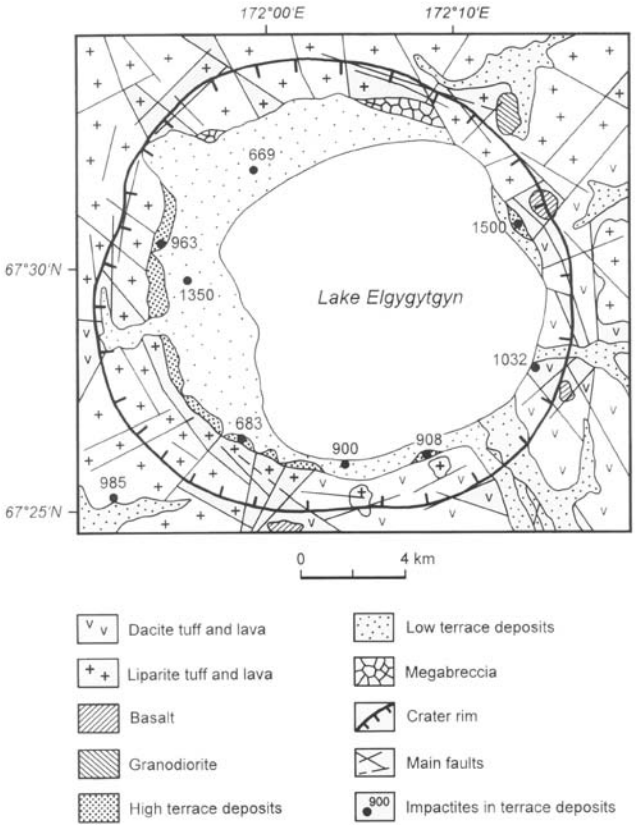


Fig. 4. Schematic geological map of the El'gygytgyn impact crater, after Gurov and Gurova (1991), with additional information (field work by E. Gurov and E. Gurova). North is up. The locations of some of the more important samples on the terraces, from which impact rocks were studied, are indicated by solid circles.

Table 1. Major element composition of volcanic rocks from the El'gygytgyn impact crater.[a]

	Ignimbrite (7)	Rhyolite tuff and lava (16)	Andesite-dacite tuff and lava (5)	Target average[b]
SiO_2	70.16	72.51	63.00	70.72
TiO_2	0.33	0.30	0.56	0.34
Al_2O_3	14.47	12.79	16.57	13.90
Fe_2O_3	1.88	1.31	3.40	1.76
FeO	1.05	0.76	1.37	0.86
MnO	0.08	0.05	0.12	0.06
MgO	0.73	0.49	1.59	0.72
CaO	2.25	1.16	3.73	2.01
Na_2O	3.03	2.21	3.29	2.57
K_2O	3.92	5.36	3.08	4.48
P_2O_5	0.08	0.07	0.14	0.10
CO_2	0.48	0.68	0.91	0.62
H_2O	0.27	0.41	0.56	0.39
Total	98.73	98.10	98.32	98.53

[a]Wet chemical analyses. Data in wt%. Numbers in parentheses give the number of samples analyzed.

[b]Target average composition was calculated in accordance with the relative thickness of the main volcanic rock types in the strata of the basement rocks of the crater.

Ignimbrites and tuffs of rhyolites and dacites are the most abundant rock types of the crater basement. The composition of the ignimbrites is given in Table 2. Mineral clasts and fragments of those rocks are quartz, orthoclase ($Or_{80}Ab_{20}$ to $Or_{60}Ab_{40}$), and plagioclase (An_{20} to An_{30}). The refractive indices of unshocked orthoclase are n_γ = 1.526–1.529, n_α = 1.520–1.523, and birefringence of 0.006–0.007 and of plagioclase are n_γ = 1.548–1.553, n_α = 1.542–1.547, and birefringence of 0.006. Mafic minerals are biotite and, rarely, amphibole. The fine-grained matrix of lavas and tuffs consists of quartz and feldspars. Andesites and andesite tuffs contain fragments and clasts of andesine (An_{45} to An_{40}), clinopyroxene, and amphibole.

SAMPLES AND ANALYTICAL METHODS

Samples

The samples for this study were collected by E. Gurov and E. Gurova during expeditions to the El'gygytgyn crater from 1977 to 1980. All types of impact rocks are redeposited on the terraces of the El'gygytgyn Lake. The samples of unshocked volcanic rocks of the crater target were collected at the crater rim, the inner walls, and the outer slopes of the structure.

Apart from samples described by Gurov and Gurova (1991), the following samples were studied specifically for this paper:

- El-669-8 (impact melt rock): Dark gray vesicular devitrified glass with abundant inclusions of minerals and glass clasts. Mineral inclusions are predominantly shocked quartz and lechatelierite. Greenish-gray, brown and black glass clasts, up to 4 cm in diameter, in sharp contact with the melt.
- El-669-10 (impact melt rock): Contains abundant lithic and mineral clasts and glass fragments. The impact glass shows a fluidal texture with vesicles up to 1 mm in diameter. Clasts, ≤2 mm in diameter, are strongly shocked volcanic rocks and glasses. Mineral inclusions are shocked quartz and lechatelierite.
- El-669-5 (partly melted rhyolite): Gray fluidal vesicular heterogeneous glassy matrix with relics of quartz phenocrysts. Quartz is converted into transparent diaplectic glass with coesite veinlets. Remnants of black homogenous impact melt occur on clast surfaces.
- El-985-91 (glass bomb): 11 × 21 mm in size. Dark fluidal transparent glass with bands of brown glass. Rare mineral clasts are lechatelierite and shocked quartz.
- El-689 (glass bomb): Aerodynamically shaped bomb. The glass is semitransparent and dark colored. It contains very rare lechatelierite clasts up to 0.3 mm in diameter. Rare vesicles are up to 1 mm in diameter.
- El-699 (glass bomb): This sample is very similar to the previous one. Glass is semitransparent and shows fluidal texture. Inclusions comprise shocked quartz and lechatelierite. Vesicles occur in the rim parts of the bomb.

Experimental Methods

Petrographic and mineralogical investigations of impact rocks were carried out by optical microscopy. Shock metamorphic effects of siliceous volcanic rocks were studied (Gurov and Gurova 1979, 1991), and the orientation of planar deformation features (PDFs) in quartz was determined using a four-axis universal stage. Refractive indices of quartz and feldspars were measured with immersion liquids to estimate shock pressures using the data presented by Stöffler and Langenhorst (1994). The presence of high pressure phases of silica and some other minerals was determined by X-ray diffractometry. To detect stishovite and coesite, fractions of shocked quartz were dissolved in hydrofluoric acid.

The chemical composition of impact rocks and basement rocks was determined by wet chemical methods at the Institute of Geological Sciences of the Ukraine. Splits of unaltered impact rocks were carefully selected under a binocular microscope. The composition of minerals was analyzed by electron microprobe analysis using a Camebax instrument at the Institute of Geological Sciences of the Ukraine (cf. Gurov and Gurova 1991).

Concentrations of major elements, V, Cu, Y, and Nb, on the new samples were measured on powdered samples by standard X-ray fluorescence (XRF) procedures (see Reimold et al. [1994] for details on procedures, precision, and accuracy). All other trace elements were analyzed by instrumental neutron activation analysis (INAA; see Koeberl [1993] for details). For most samples, Sr and Zr

Table 2. Chemical composition of ignimbrites of the El'gygytgyn impact crater.[a]

	616-b	649	781	925	945	963-a	974	Average
SiO_2	68.20	71.46	67.78	70.01	70.50	70.65	72.50	70.38
TiO_2	0.41	0.14	0.46	0.29	0.34	0.37	0.31	0.36
Al_2O_3	13.04	13.72	15.49	14.68	14.80	15.68	13.85	14.47
Fe_2O_{3tot}	2.45	1.50	2.75	1.77	1.33	2.11	1.23	1.85
FeO	1.25	0.72	0.72	1.43	1.15	0.93	1.15	1.05
MnO	0.14	0.14	0.07	0.03	0.09	<0.01	0.09	0.08
MgO	0.96	0.61	1.06	0.78	0.78	0.32	0.62	0.73
CaO	3.61	2.54	2.73	1.91	2.04	1.26	1.68	2.25
Na_2O	3.40	2.98	3.06	3.10	3.17	2.40	3.15	3.03
K_2O	3.68	4.41	3.60	4.11	3.88	3.74	4.00	3.92
P_2O_5	0.12	0.05	0.11	0.06	0.08	<0.01	0.12	0.08
CO_2	0.88	0.44	0.24	0.88	0.14	0.46	0.34	0.48
H_2O	0.54	0.20	0.12	<0.01	0.55	0.16	0.35	0.27
LOI	1.05	0.48	1.62	1.13	1.00	1.56	0.58	1.29
Total	99.74	99.56	99.60	99.61	99.52	99.64	99.56	–

[a]Wet chemical analyses; data are in wt%. Samples: 616-b: lava-like porphyric rock with fragments of plagioclase, orthoclase, quartz, biotite, and amphibole in fine-grained fluidal glass. Lenticular inclusions of brown fluidal tuff and lava occur in the rock; 649: porphyric rock with fragments and clasts of quartz, plagioclase, orthoclase, biotite, and amphibole in fine-grained recrystallized matrix that partly preserves fluidal structure. Flattened particles of tuff and lava do not have sharp contacts with matrix; 781: as 649; 945: lava-like porphyric rock with fluidal fine-grained matrix and fragments of quartz, feldspars, biotite, and, rarely, amphibole. Rare lenticular inclusions of tuff and lava of the same composition are present in the rock; 963-a: as 945; 974: lava-like rock with xenoliths of brown flattened particles of tuff and phenocrysts of plagioclase, orthoclase, quartz, and biotite. Matrix is recrystallized in fine-grained matter but preserves fluidal structure.

concentrations were determined by both XRF and INAA, and for some of the low abundance samples, Ni data were also obtained by XRF. Iridium was measured with γ-γ multiparameter coincidence spectrometry (see Koeberl and Huber [2000] for details).

SHOCK METAMORPHISM OF VOLCANIC ROCKS OF THE EL'GYGYTGYN IMPACT CRATER

Impact rocks are exposed at the El'gygytgyn crater at the present-day erosional level only in redeposited state. Impact melt rocks, glasses, and shock-metamorphosed volcanic rocks occur in deposits of lacustrine terraces inside the crater basin and, rarely, in alluvial deposits of some streams on the outer slopes of the crater rim (Fig. 5). The source of these deposits was the ejecta on the crater rim and its slopes. The sizes of impact rock clasts are mainly to 5–10 cm, and only rare lumps of impact melt rocks are up to ~1 m in diameter.

Shock-metamorphosed volcanic rocks are tuffs, ignimbrites, and lava of rhyolites and dacites, rarely andesites and andesite tuffs. Clasts of impact rocks have predominantly irregular shapes, while partly impact-melted volcanic rocks have aerodynamically shaped forms. Remnants of vesicular impact melt on the surface of some rock clasts indicate that their source rocks were suevites and impact melt breccia. All rocks are fresh, and only limited weathering is observed in a few rare cases.

The classification of the shock-metamorphosed crystalline rocks of Stöffler (1971) was used for the description of the shocked volcanic rocks of the El'gygytgyn structure, while considering some peculiarities of porphyric rocks and tuffs. Shock-metamorphic effects are more distinct in phenocrysts in porphyric rocks and mineral clasts in tuffs, while shock metamorphism of the fine-grained matrix is less noticeable until selective melting occurs (Gurov and Gurova 1979, 1991).

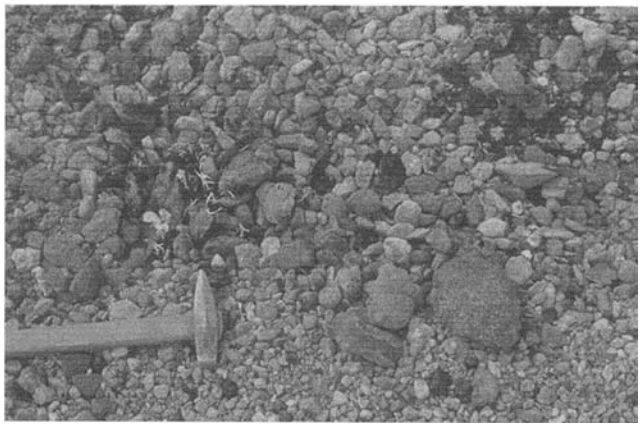


Fig. 5. Accumulation of impact glasses (dark gray to black) and clasts of shock metamorphosed volcanic rocks (gray to light gray) on a lacustrine terrace at the southeastern shore of Lake El'gygytgyn (site 908). Aerodynamical shapes of some glass bodies and partly melted volcanic rocks are visible.

In the following sections, we describe the characteristics of the rocks representing the various shock stages that we studied.

Stage I (Shock Pressures up to 35 GPa)

At shock pressures ≤28 GPa, weakly to moderately shocked rhyolite clasts are somewhat fractured; at the

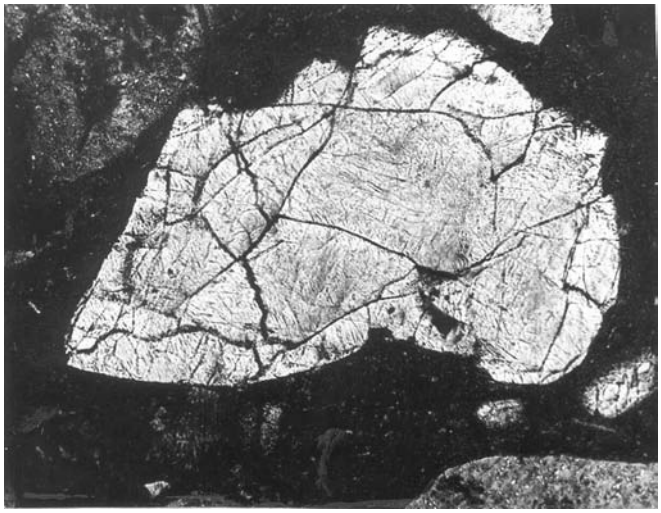


Fig. 6. Clast of shocked quartz in rhyolite. Irregular rough fractures and multiple PDFs occur in quartz (sample 1032-7, 2.0 mm wide, crossed polarizers).

macroscopic scale, it is difficult in some cases to distinguish them from unshocked rocks. The quartz contains planar fractures (PFs) and PDFs (Fig. 6). The predominant PF orientation is parallel to $\{10\bar{1}1\}$, rarely to $\{10\bar{1}4\}$, $\{22\bar{4}1\}$, and $\{10\bar{1}3\}$, while the PDF orientations are parallel to $\{10\bar{1}3\}$, $\{10\bar{1}4\}$, $\{10\bar{1}1\}$, $\{11\bar{2}2\}$, $\{11\bar{2}2\}$, $\{51\bar{6}1\}$, and $\{22\bar{4}1\}$. The refractive indices of $\{22\bar{4}1\}$ quartz are slightly lowered to n_e = 1.548–1.550 and n_o = 1.540–1.541, and the birefringence is 0.008–0.009, corresponding to shock pressures of up to 28 GPa according to Stöffler (1974) and Stöffler and Langenhorst (1994). Coesite and stishovite were not found. The refractive indices of orthoclase are lowered to n_β = 1.516–1.521 and n_α = 1.511–1.515. Polysynthetic twins are preserved in plagioclase, with refractive indices of n_β = 1.527–1.533 and n_α = 1.522–1.527. Kink bands are abundant in biotite.

Significant changes of volcanic rocks occur at higher shock pressures. Open fractures (up to 1 mm wide) occur in the tuff clasts. The fracture volume increases from 1.5 to 7 vol%, derived from counting in thin sections. The refractive indices of quartz fragments and clasts are strongly reduced to 1.475–1.494, and birefringence is about 0.002–0.003, corresponding to shock pressures in the range of 28 to 35 GPa (Stöffler 1974; Stöffler and Langenhorst 1994). PDFs are abundant in quartz (Fig. 7), with up to 12 sets of PDFs occurring in some phenocrysts. The predominant orientation is $\{10\bar{1}2\}$, while $\{10\bar{1}4\}$, $\{10\bar{1}3\}$, $\{11\bar{2}2\}$, $\{21\bar{3}1\}$, $\{40\bar{4}1\}$, and $\{10\bar{1}0\}$ are less common. The presence of stishovite and coesite was determined by X-ray powder diffractometry of heavily shocked opalescent quartz from two samples of rhyolite tuff. A fraction of pure stishovite (main X-ray reflections at 0.296 and 0.153 nm) was obtained after quartz was dissolved in hydrofluoric acid (Gurov et al. 1979a). Potassium feldspar contains up to two systems of PDFs and has lowered refractive indices: n_β = 1.512–1.514, n_α = 1.509–1.511, and the birefringence is ~0.003. Oligoclase contains several sets of PDFs; its refractive indices are lowered to n_β = 1.525–1.530 and n_α = 1.520–1.526, but polysynthetic twins are still preserved. Biotite grains are partly replaced by opaque minerals, which, according to X-ray powder patterns, comprise magnetite.

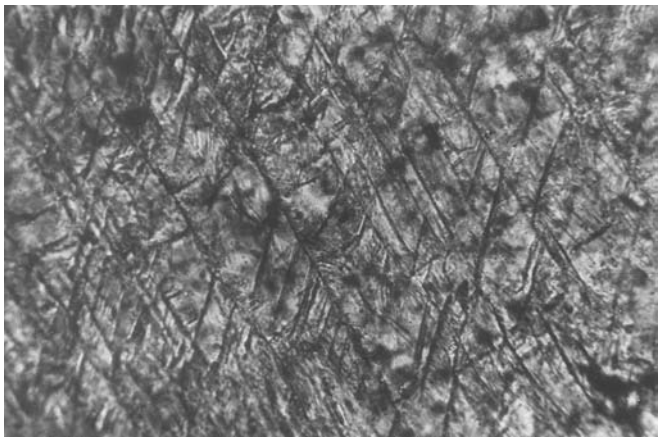


Fig. 7. Multiple PDFs in shocked quartz from rhyolite tuff (sample 699-A, 0.9 mm wide, crossed polarizers).

Stage II (Shock Pressures from 35 GPa to 45 GPa)

Samples of tuffs have open fractures up to 1 mm wide. Quartz and potassium feldspar fragments and clasts are transformed into diaplectic glasses. Diaplectic quartz glass is transparent (Fig. 8); its refractive indices range from 1.462 to 1.468. X-ray diffraction patterns with only one weak diffusion line at d = 0.335 nm confirm the amorphous state. Thin semi-translucent zones and veinlets often intersect grains of diaplectic quartz glass (Fig. 9). The zones are of complex structure and are composed of coesite segregations in central parts of veinlets, while the outer parts are composed of secondary quartz. Individual coesite grains (n_z = 1.594, n_x = 1.590, birefringence of 0.004) within the segregations are from 1 to 25 μm in diameter. After treatment with hydrofluoric acid, the remnant showed the X-ray powder pattern of pure coesite (main reflections: d = 0.344, 0.310, 0.171 nm). No stishovite was observed in diaplectic quartz glass from the El'gygytgyn crater. Grains of potassium feldspar in tuffs and lavas preserve their initial shapes but are converted into transparent diaplectic glass with rare spherical vesicles up to 0.05 mm in diameter (Fig. 10). While quartz and potassium feldspar are converted into diaplectic glasses, plagioclase in the same sample mainly preserves the properties of the crystalline phase. Relics of polysynthetic twins occur in this mineral. The refractive indices of plagioclase are lowered to n_β = 1.524–1.528 and n_α = 1.520–1.524, with birefringence of 0.004. Full isotropization of plagioclase was observed in several tuff samples, where clasts are converted into translucent isotropic glass with rare voids.

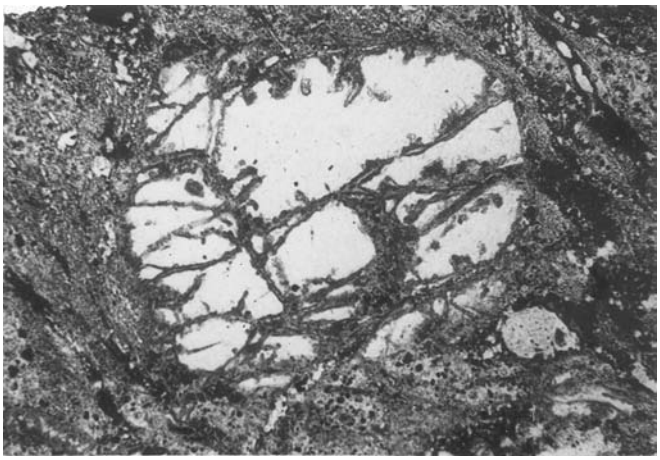


Fig. 8. Strongly shocked rhyolite tuff. Grain of transparent diaplectic quartz glass with the veinlets of coesite and secondary quartz. The matrix is melted and converted into inhomogeneous fluidal glass (sample 908-7B, 1.9 mm wide, parallel polarizers).

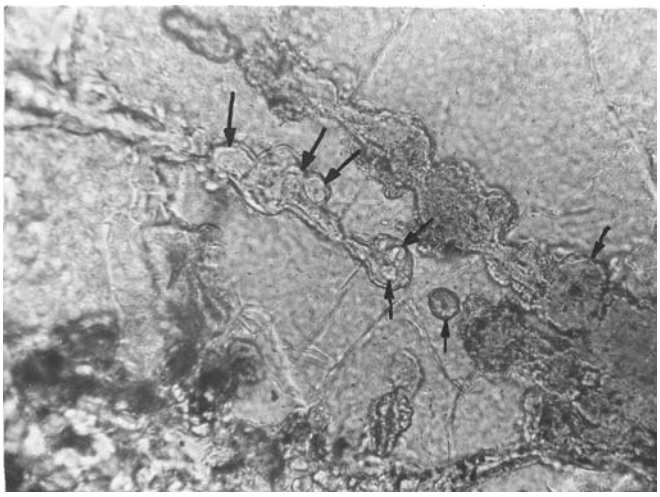


Fig. 9. Segregations of coesite and secondary quartz in diaplectic quartz glass. Coesite forms grains with high relief in central parts of clustered veinlets (black arrows), while their peripheral zones are fine-grained aggregates of secondary quartz (sample 908-7B, 0.65 mm wide, parallel polarizers).

The refractive indices of the glass range from 1.513 ± 0.001 to 1.517 ± 0.002. The composition of these maskelynites is about An_{27} to An_{36}, using a diagram compiled by Stöffler (1974) as reference. Biotite is replaced by ore minerals. The matrix of the porphyric rocks and tuffs is isotropic.

Rare clasts of strongly shocked andesites occur in the terrace deposits. They contain phenocrysts of plagioclase, orthopyroxene, and amphibole. Plagioclase phenocrysts preserve their initial shapes but are converted into transparent diaplectic glass. Phenocrysts of pyroxene are intensely twinned.

Stage III (Shock Pressures from ~45 to ~55 GPa)

Partly melted volcanic rocks belong to this stage. They

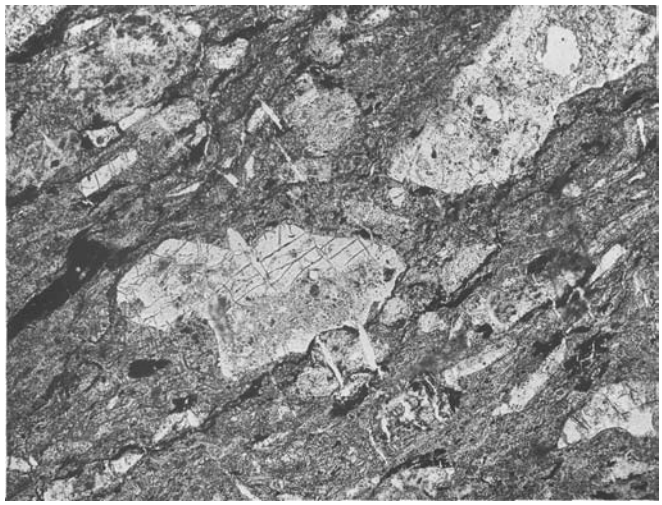


Fig. 10. Two grains of diaplectic potassium feldspar glass (center and upper right) in strongly shocked tuff. The minerals in matrix preserve their initial shapes but are mainly diaplectic glasses. The fluidal textures of matrix testify about the beginning of shock melting (sample 908-11B, 2.8 mm wide, parallel polarizers).

are widespread in terrace deposits inside the El'gygytgyn crater; a few also occur in nearby areas just outside the crater rim. Volcanic rocks shocked at this stage are vesicular pumice-like rocks of low density, some of which float in water. The clasts often have aerodynamic forms. Transparent diaplectic quartz glass with refractive indices from 1.462 to 1.467 contains veinlets and irregular segregations of coesite, which is more abundant in outer parts of the grain. Potassium feldspar and plagioclase are converted into irregular to lens-shape vesicular, colorless melt glasses. The refractive indices range from 1.488 to 1.490 for potassium feldspar glass and from 1.505 to 1.515 for plagioclase glasses. The contacts of feldspar glasses with fused matrix range from sharp to gradual. The matrix of porphyric rocks and tuffs comprises inhomogeneous fluidal vesicular glass with refractive indices from 1.485 to 1.515. Abundant spherical inclusions with a refractive index of ~1.590 are probably coesite, as the X-ray patterns of these glasses contain a weak reflection at d = 0.310 nm.

Stage IV

At shock pressures exceeding ~55 GPa, impact melt rocks and impact glasses are formed. These rocks are described in the next section.

IMPACT MELT ROCKS AND GLASSES OF THE EL'GYGYTGYN CRATER

Impact melt rocks and impact melt breccias occur in terrace deposits within the crater basin but were not found outside of the crater. These rocks were probably derived from flows and pools of impact melt on the crater rim and wall,

similar to the distribution of impact melt flows in some lunar craters (Hawke and Head 1977). Fragments of impact melt rocks have irregular angular forms and range in size from several cm to 1 m. Black and dark gray impact melt rocks consist of vesicular glass with abundant clasts of shocked volcanic rocks, minerals, and glasses. Fragments of dark green, brown, and gray glasses are in sharp contact with the rock matrix. Clasts of volcanic rocks predominantly show high stages of shock metamorphism. The matrix of the impact melt rocks consists of partly devitrified vesicular glass with refractive indices ranging from 1.500 to 1.515 for fresh glass and up to 1.520 for devitrified glass. Microlites of orthopyroxene (Fig. 11) and, in some cases, of albite occur in glass (Gurov and Gurova 1991). The compositions of the impact melt rocks (Table 3) are very similar to the average composition of the target rocks.

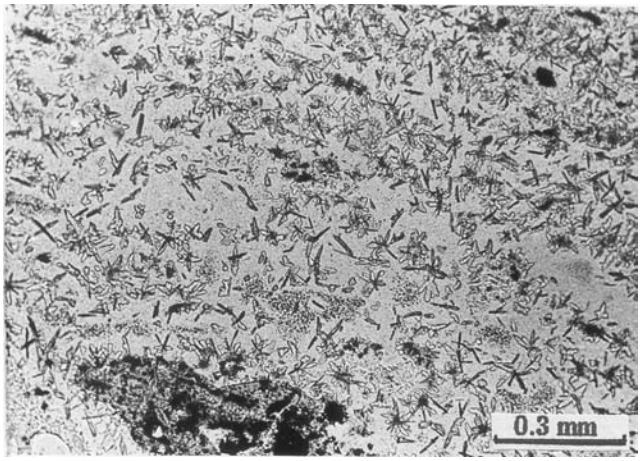


Fig. 11. Impact melt glass with glassy matrix and prismatic orthopyroxene microlites. The areas of opaque glass are extensively devitrified. The fragments (bottom left) are vesicular lechatelierite and shock-metamorphosed volcanic rock (sample 985-60, 2.2 mm wide, parallel polarizers).

The inner surface of vesicles in impact melt rocks are, in some cases, covered with thin (≤0.2 mm) layers of transparent (colorless) glass. Transparent clusters of this glass, up to 2 mm in size, occur on the surface of the voids. The formation of this glass by condensation of silicate vapor has been suggested by Gurov and Gurova (1991), as no evidence of hydrothermal activity has been seen in the shocked rocks of the crater.

Abundant glass bombs occur in the terrace deposits of the El'gygytgyn crater together with shock-metamorphosed rocks and massive impact melt rocks. While impact melt rocks occur only inside the crater basin, glass bombs are also found outside the crater in terrace deposits of some streams. The bombs have aerodynamical forms, including drops, ropes, cakes, and cylinders, and are rarely of irregular shape (Fig. 12). The bomb surfaces are rough and without luster, and rounding during late-stage transportation by water is rare. Bomb diameters commonly range from 1 to 15 cm. Their weight varies mostly from 3 to 400 g, but some large bodies up to 2 kg were also found. The density of the glass ranges from 2.40 ± 0.05 to 2.50 ± 0.05 g/cm^3. The

Table 3. Chemical composition of impact melt rocks of the El'gygytgyn impact crater.[a]

	651-b	651-5	669-10	669-20	678-I	900-11	900-12	900-13	Average
SiO_2	67.68	67.92	70.50	69.65	70.40	69.64	69.62	68.42	69.23
TiO_2	0.30	0.39	0.31	0.34	0.26	0.31	0.31	0.31	0.32
Al_2O_3	15.63	15.29	14.56	15.08	15.07	15.52	15.03	15.43	15.20
Fe_2O_3	0.81	0.79	1.02	1.33	1.33	1.41	1.41	1.21	1.16
FeO	2.15	2.53	1.72	1.65	1.58	1.97	1.79	2.15	1.94
MnO	0.07	0.08	0.10	0.07	0.10	–	0.12	0.12	0.08
MgO	1.19	1.09	0.77	0.95	0.61	0.68	0.78	0.91	0.87
CaO	2.87	2.40	1.88	2.40	2.11	2.28	2.18	3.27	2.42
Na_2O	3.00	3.14	2.49	3.10	2.75	2.28	2.18	3.27	2.78
K_2O	3.83	3.83	4.90	3.29	4.42	3.88	4.17	3.62	3.99
P_2O_5	0.16	0.16	0.03	0.09	0.05	0.06	0.06	0.08	0.09
SO_3	tr.	tr.	0.02	tr.	0.01	tr.	tr.	tr.	tr.
CO_2	n.d.	n.d.	0.46	0.38	0.24	0.44	0.44	0.44	0.40
H_2O^-	0.30	0.22	0.25	0.30	0.22	0.12	0.08	0.10	0.19
LOI	2.29	2.58	0.62	1.04	1.03	0.28	0.69	0.66	1.14
Total	100.28	100.42	99.63	99.67	100.18	98.87	98.86	99.99	99.81

[a]Wet chemical analyses; data in wt%; tr = traces (<0.01 wt%); n.d. = not determined. Samples: 651-b: impact melt rock is vesicular devitrified glass with rare zones of black fresh glass. Devitrified glass contains microlites of pyroxene and spherulitic aggregates of prismatic microlites of plagioclase; 651-5: as 651-b, clasts of ballen quartz; 669-10: vesicular and porous impact melt breccia composed of gray devitrified glass and xenoliths of colorless highly vesicular glass and diaplectic quartz glass. Breccia matrix is glass with abundant microlites of pyroxene and feldspar; 669-20: as 669-10, matrix is vesicular devitrified glass; 678-I: impact melt breccia with numerous xenoliths of vesicular glass and highly shocked volcanic rocks. Matrix is highly recrystallized glass with spherulitic segregations of feldspars; 900-11: impact melt rock with microlites of pyroxene in glass matrix. Dark brown bands and spots of devitrification underlie fluidal structure of glass; 900-12: fluidal impact melt rock with lithic fragments of vesicular glasses, shock-metamorphosed rocks, and mineral clasts. Melt rock has fluidal texture and contains microlites of pyroxene and brown devitrification zones; 900-13: strongly devitrified impact melt breccia with xenoliths of glass and diaplectic quartz glass. The fluidal vesicular matrix consists of pyroxene and feldspar microlites cemented by gray-brown devitrified glass. Diaplectic quartz glass contains coesite inclusions.

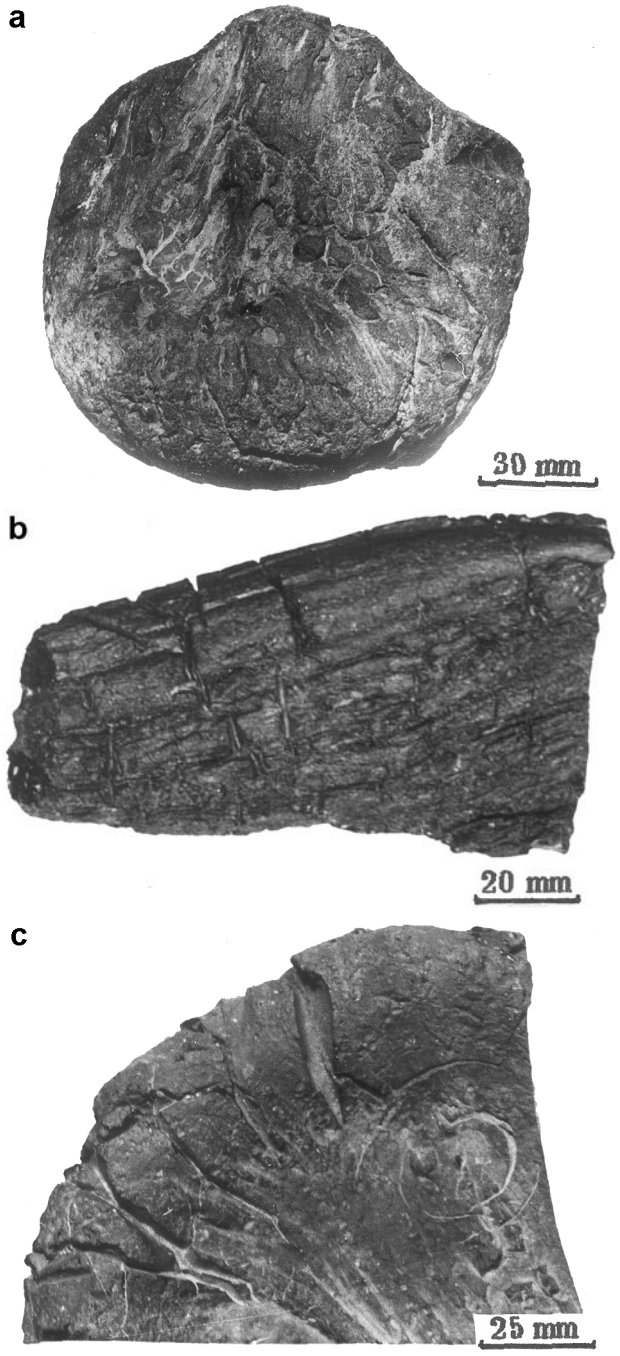


Fig. 12. Form of aerodynamically shaped glass (bombs). All bombs have shiny black surfaces: a) teardrop-shaped bomb, 7 × 12 × 12 cm (sample 689-1); b) elongated glass bomb, 4 × 6 × 11 cm, with striated relief and deep transversal cracks (sample 689-12); c) fragment (6 × 10 × 12.5 cm) of disk-shaped glass bomb with deep radial cracks, (sample 985-98).

density of vesicular glass is lower at about 2.35 g/cm^3. The color of glass is black, rarely dark gray, in hand samples and colorless to pale yellow in thin section. Bands of brown glass enhance its fluidal structure (Fig. 13). Gas bubbles up to a few mm in diameter occur within the glass. The

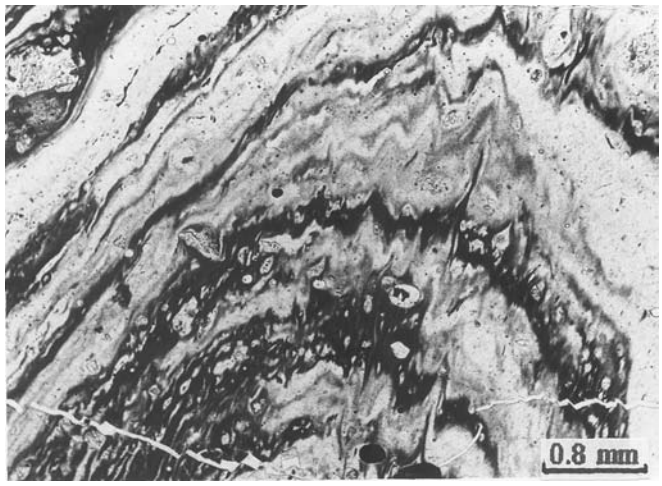


Fig. 13. Fluidal structure of inhomogeneous glass (sample 690, 3.5 mm wide, parallel polarizers). Distorted layers of brown glass show flow during melting.

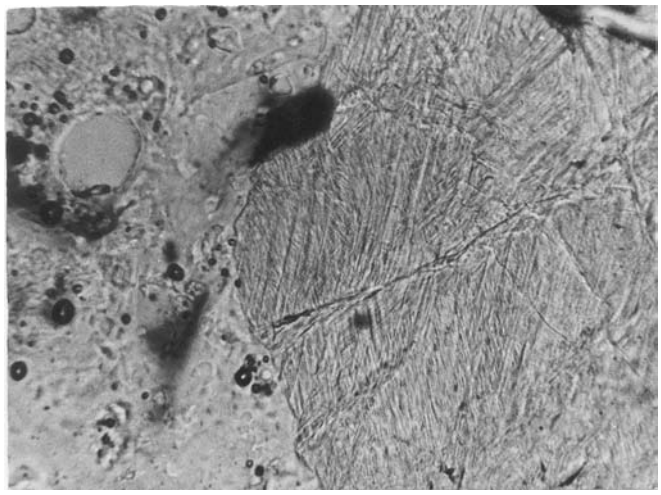


Fig. 14. Shocked quartz with multiple PDFs in vesicular glass (sample 918, 2.1 mm wide, parallel polarizers).

refractive indices vary mostly from 1.505 to 1.515 but reach 1.540 in brown glass. The glass is fresh, and its devitrification is rare. The mineral inclusions in glass are shocked quartz (Fig. 14), as well as diaplectic quartz glass and lechatelierite (Fig. 15). Rare inclusions in the form of isolated spherical grains or clusters are magnetite, titanomagnetite, and ilmenite. Microprobe analyses of titanomagnetite grains show TiO_2 contents from 5.4 to 11.8 wt% and Al_2O_3 contents up to 6.6 wt%.

Deep open cracks, ranging from 1 to 5 mm in width and 1 to 7 mm in depth, are the main characteristics of the bomb surface morphology (Fig. 12). The cracks formed during the contraction of the melt by cooling and solidification during their transport in the atmosphere. It is assumed that the volume of open cracks corresponds to a decrease in melt volume from the beginning of glass formation to its

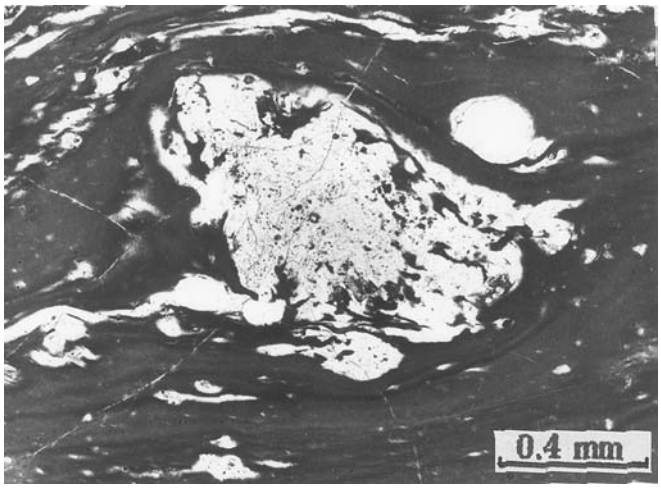


Fig. 15. Transparent lechatelierite inclusion in brown fluidal glass. The lechatelierite (center) has sharp contacts with the surrounding glass (sample 652-25, 1.7 mm wide, parallel polarizers).

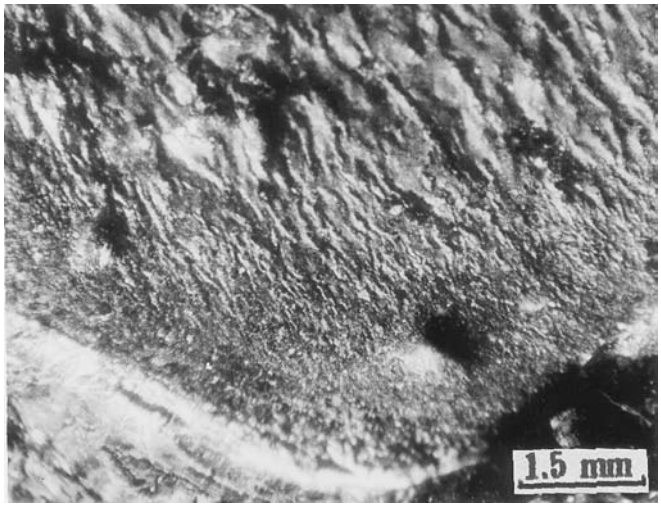


Fig. 16. Striated relief of glass bomb surface. Traces of ablation are absent behind the step (dark area in the lower part of image) and appear at a distance of about 2 mm from it (sample 985-89, 10.5 mm wide). This image illustrates secondary melting of the bomb surface during transportation in the atmosphere.

solidification. The volumes of open cracks of 25 bombs from 5 to 12 cm in diameter were determined as the difference between bomb volumes with filled and with open empty cracks. For this purpose, the cracks were filled with paraffin. The open cracks equal from 0.45 to 3.67% of the whole bomb volume. Bombs with a crack volume from 1.0 to 1.5% predominate. A decrease of 1.0–1.5 vol% in melt volume corresponds to a temperature drop of about 300–450 °C from the beginning of the formation of the glass crust to its solidification.

Traces of ablation and secondary melting are visible on the surface of eight bombs out of 160 that were studied. These bombs have drop shapes and are from 4.0 × 5.0 × 6.9 cm to 7.3 × 10.3 × 11.0 cm in size. The ablation is indicated by striated relief on the frontal and lateral surface of the bombs. Open bubbles that are cut by ablation, to about 3 mm in diameter, occur on the lateral surface of those bombs. Secondary melting is visible on the inner walls of some open cracks. Positive surface relief protected some areas of the bomb surface from ablation. A striated relief appears some mm behind the steps on the bomb surface (Fig. 16). The maximal thickness of ablation and secondary melting zones approaches 1 mm. According to O'Keefe (1978), a thickness of an ablated glass zone of about 2 mm corresponds to an entrance velocity of the bomb into the dense atmosphere of about 5 km/s. The occurrence of bombs at a distance of about two crater radii from the crater center indicates subvertical trajectories. The following history of those bombs' formation is indicated: 1) ejection of melt from the crater; 2) formation of aerodynamically shaped bombs; 3) solidification of the surfaces of the bombs during flight along upward and downward trajectories; 4) ablation and secondary melting of the bomb surface during re-entrance into the denser parts of the atmosphere; 5) falling of bombs on the surface. The absence of local rock fragments attached to the surface of the bomb indicates that their surfaces were already solid when they hit the surface.

Glass bombs from eight different areas of the El'gygytgyn impact crater show only a limited range in chemical composition (Tables 4 and 5). The SiO_2 content varies from 68.60 to 71.48, Na_2O from 2.66 to 3.16, and K_2O from 3.30 to 4.37 wt% (Gurov and Gurova 1991; Feldman et al. 1982). The composition of the glass bombs is similar to the calculated average composition of the target (Table 1), but the closest agreement is to the composition of the rhyolite ignimbrites of the uppermost horizon of volcanic strata in the crater area (Table 2). We assume that these rhyolite ignimbrites were the main source material for melt bomb formation during the earliest stage of impact melting of the target. One main characteristic of the glass composition is the low Fe_2O_3/FeO ratio due to reduction in high temperature melts.

In addition to the major element data report here, we studied three glass bombs, two impact melt rocks, and one sample of selectively melted rhyolite for their trace element composition (Table 4). Their major element composition (newly measured by XRF) is similar to that of target volcanic rocks (cf., Table 1). The trace element contents show a limited variation. A chondrite-normalized REE diagram for selected samples of impact glass is presented in Fig. 17. It shows that the melt rock samples, melt bombs, and the rhyolite have basically identical composition; no evidence for a post-formational hydrothermal alteration is seen. Compared to the one rhyolite sample, the siderophile element content of the melt bombs is not very high; only the Cr content is significantly higher, while the Co and Ni abundances show hardly any difference. The iridium content in these samples ranges from 24 ppt in the glass bomb to 74 and 111 ppt in impact melt rocks, which are not high values compared to those that have been

Table 4. Composition of selected impactites from the El'gygytgyn impact crater.[a]

	EL 669-5 rhyolite (pm)	EL 669-8 IMR	EL 669-10 IMR	EL 689 glass bomb	EL 699 glass bomb	EL 985 glass bomb
SiO_2	71.55	68.99	69.56	71.91	71.62	70.50
TiO_2	0.40	0.39	0.38	0.36	0.42	0.38
Al_2O_3	13.38	14.75	15.32	14.23	15.21	15.41
Fe_2O_3	3.11	3.13	2.92	2.94	3.00	3.23
MnO	0.08	0.09	0.09	0.09	0.09	0.11
MgO	1.23	0.84	1.09	1.03	1.20	1.17
CaO	2.56	2.69	2.47	2.32	2.68	2.68
Na_2O	2.93	3.31	2.98	2.74	2.17	2.72
K_2O	3.66	3.56	4.01	3.91	3.94	4.00
P_2O_5	0.08	0.11	0.12	0.08	0.08	0.08
LOI	1.45	1.24	1.36	0.20	0.06	0.08
Total	100.43	99.10	100.30	99.81	100.47	100.36
Sc	7.58	8.14	13.1	8.45	8.15	9.58
V	33	33	34	–	–	36
Cr	8.1	31.2	46.1	20.6	45.1	33.2
Co	4.53	4.71	4.41	5.16	5.89	5.04
Ni	29	8	12	21	16	11
Cu	<2	<2	<2	<2	<2	<2
Zn	61	71	68	120	173	52
Ga	10	10	20	26	22	25
As	7.07	8.06	5.11	2.08	2.91	3.41
Se	0.16	0.32	0.26	0.26	0.44	0.24
Br	0.6	0.5	0.6	0.7	0.4	0.4
Rb	150	148	155	165	145	155
Sr	273	324	260	195	225	242
Y	33	27	31	<10	<10	34
Zr	210	205	200	221	175	230
Nb	11	11	12	<8	<8	13
Sb	0.65	1.23	0.94	0.85	0.64	1.45
Cs	5.97	8.93	7.57	9.09	7.11	9.54
Ba	780	800	850	870	840	830
La	37.5	42.5	45.5	40.8	37.1	40.8
Ce	70.8	77.1	88.3	75.1	66.9	74.9
Nd	34.1	34.8	43.9	34.9	31.6	35.9
Sm	5.68	6.04	8.04	5.96	5.25	6.35
Eu	1.09	0.98	0.98	1.02	0.93	1.03
Gd	6.2	5.5	6.5	5.1	4.9	5.2
Tb	0.91	0.8	1.12	0.85	0.76	0.88
Tm	0.47	0.43	0.57	0.42	0.41	0.53
Yb	2.93	2.99	3.91	2.99	2.78	3.25
Lu	0.45	0.49	0.63	0.47	0.44	0.49
Hf	5.87	5.85	6.29	5.81	4.96	5.82
Ta	0.76	0.86	0.81	0.88	0.74	0.76
W	1.3	0.9	1.2	0.7	0.9	0.9
Ir (ppt)	n.d.	111 ± 21	73 ± 17	24 ± 10	n.d.	n.d.
Au (ppb)	0.6	0.9	0.3	0.5	0.2	0.4
Th	16.4	17.3	16.2	17.3	14.7	15.9
U	4.81	4.69	4.08	4.25	3.75	4.26
K/U	6341	6326	8190	7667	8756	7825
Zr/Hf	35.8	35.0	31.8	38.0	35.3	39.5
La/Th	2.29	2.46	2.81	2.36	2.52	2.57
Hf/Ta	7.72	6.80	7.77	6.60	6.70	7.66
Th/U	3.41	3.69	3.97	4.07	3.92	3.73
La_N/Yb_N	8.65	9.61	7.86	9.22	9.02	8.48
Eu/Eu*	0.56	0.52	0.41	0.57	0.56	0.55

[a]Major elements in wt%; trace elements in ppm, except as noted; all Fe as Fe_2O_3. IMR = impact melt rock; (pm) = partially melted; for a detailed sample description, see text.

Table 5. Chemical composition of impact melt glasses of the El'gygytgyn impact crater.[a]

	652	689-2	689-3	699-1	699-2	699-34	908-9	985-8	985-92
SiO_2	69.90	68.60	70.44	68.60	69.99	69.84	69.46	69.50	70.35
TiO_2	0.29	0.38	0.36	0.35	0.38	0.39	0.42	0.47	0.41
Al_2O_3	14.41	15.34	15.08	15.24	15.31	15.39	15.76	15.84	14.66
Fe_2O_3	1.28	1.20	0.80	1.23	0.61	0.67	0.54	1.07	0.75
FeO	2.56	2.50	2.30	3.08	2.51	2.37	2.62	2.37	2.48
MnO	0.06	0.08	0.07	0.12	0.08	0.08	0.08	0.11	0.07
MgO	0.69	1.35	1.10	1.27	1.40	1.40	1.40	1.77	1.34
CaO	2.70	2.97	2.61	2.75	2.96	3.14	2.90	3.13	2.57
Na_2O	3.16	2.96	3.04	2.88	2.70	2.72	2.66	2.82	2.88
K_2O	4.37	3.85	3.80	3.60	3.57	3.47	3.30	3.66	3.88
P_2O_5	0.04	0.09	0.06	0.08	0.06	0.07	0.07	0.12	0.07
CO_2	–	0.04	0.07	–	0.07	0.17	0.21	–	–
H_2O	0.06	0.28	tr.	0.28	tr.	tr.	0.04	0.10	0.26
LOI	0.27	0.43	0.20	0.46	0.12	tr.	0.17	0.16	0.26
Total	99.80	100.28	99.98	99.95	99.76	99.71	99.63	100.12	99.67

[a]Wet chemical analyses; data in wt%. Samples: 652: black shiny glass, in thin section colorless transparent glass with rare inclusions of diaplectic quartz glass; 689-2: black shiny glass, colorless and transparent in thin section; 689-3: as 689-2; 699-1: black glass body with deep cracks. Colorless fresh glass with light brown bands that underlie its fluidal structure. Rare inclusions are colorless vesicular lechatelierite; 699-2: colorless fluidal glass with abundant inclusions of vesicular lechatelierite and diaplectic quartz glass; 699-34: as 699-2; 908-9: fluidal glass with xenoliths of lechatelierite and vesicular heterogeneous glasses; 985-8: colorless fluidal glass with bands of brown glass. Rare inclusions are vesicular lechatelierite; 985-92: vesicular transparent glass.

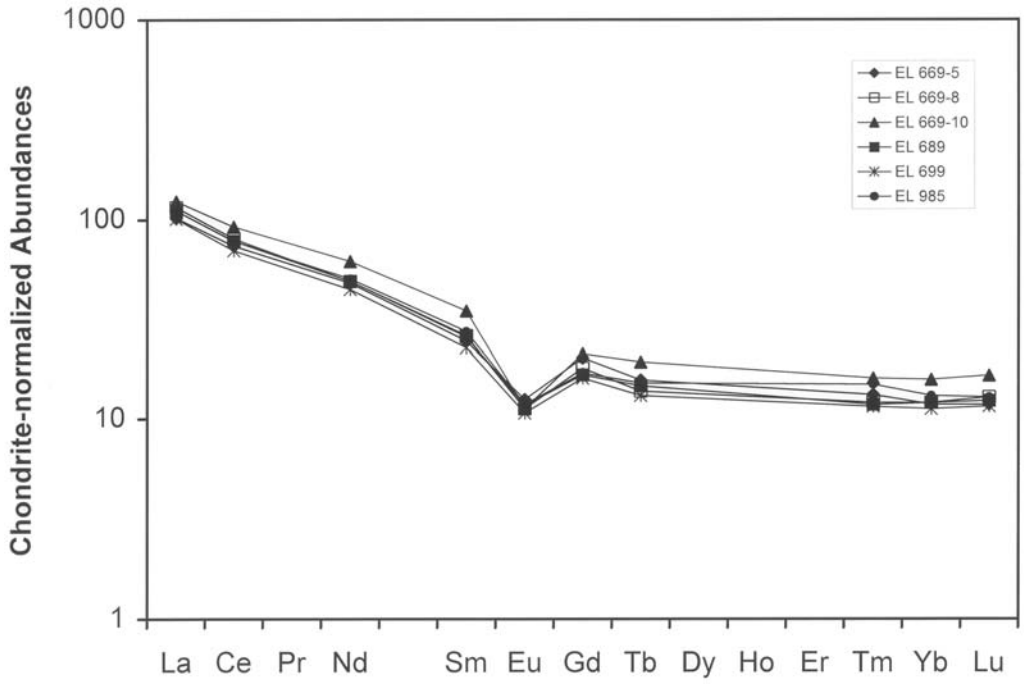


Fig. 17. Chondrite-normalized abundances of REE in impact melt rocks and a rhyolite of the El'gygytgyn crater. The normalization factors are after Taylor and McLennan (1985).

found in impact melts of other structures. However, a value of about 100 ppt Ir is somewhat elevated, but confirmation as to whether this indicates a meteoritic component will require several target rock analyses as well. At present, an achondritic projectile is the most likely interpretation of the trace element data, as most basaltic achondrites have Ni, Co, and low platinum group element contents but high Cr contents.

Glass bombs of the El'gygytgyn crater are similar in form and texture to the bombs found at some other impact structures, for example, at the Ries and Zhamanshin craters. The El'gygytgyn bombs are similar to the Ries glasses, mainly to "homogeneous glass bodies" and partly to "normal glass bombs," as described by Stähle (1972).

Some properties of the El'gygytgyn crater bombs,

including shape, traces of ablation and secondary melting, density, and refractive indices, appear similar to the characteristics of some tektites (e.g., philippinites; Chao 1963). However, the El'gygytgyn bombs formed in a smaller impact event and were not ejected as far as tektites. It can be speculated that the impact angle of the El'gygytgyn projectile was steeper than that of the tektite-forming events, resulting in more localized distributions.

SUMMARY AND CONCLUSIONS

The 18 km-diameter El'gygytgyn crater is one of the best-preserved young impact structures. The crater was formed in a series of Cretaceous volcanic rocks composed of lavas and tuffs of rhyolites, dacites, and andesites. Such a target composition is unique among terrestrial impact structures and provides the only possibility for the study of natural shock metamorphic effects in siliceous volcanic rocks.

All impactites found at El'gygytgyn so far have been redeposited; thus, none of the samples investigated here were collected in situ. Shock-metamorphosed volcanic rocks occur in the lacustrine terraces inside the crater rim and in fluviatile terraces on the outer slopes of the rim. The remnants of impact melt glass on the surface of some fragments of shocked rocks indicate that they are derived from suevites and impact melt breccias. Stishovite and coesite were found in moderately to strongly shocked rocks. Stishovite occurs in shocked quartz, while coesite is more abundant in diaplectic quartz glass. Selectively melted volcanics with shock-melted glass matrix and grains of diaplectic quartz glass are common in terrace deposits. The classification system of shock-metamorphosed crystalline rocks of Stöffler (1971) and Stöffler and Langenhorst (1994) was used to classify the shocked siliceous volcanic rocks, based on properties of quartz and feldspar and their glasses in impact rocks of the crater (Gurov and Gurova 1979). Four stages of shock metamorphism of the acid volcanic rocks are recognized:

- Stage I: Tuff and lava contain weakly to strongly shocked clasts of quartz and feldspar. Stishovite and coesite occur in quartz. Shock metamorphism of the fine-grained matrix is difficult to identify.
- Stage II: Quartz and feldspars in lava and tuff are converted into diaplectic glasses. Coesite occurs in diaplectic quartz glass. Biotite is replaced by opaques. The groundmass of the tuffs is isotropic.
- Stage III: In rocks shocked to this stage, quartz is converted into diaplectic glass, often with coesite, while feldspar clasts are melted and have an irregular or lens-like form; most of them preserve sharp contacts with the surrounding matrix, which is composed of heterogeneous vesicular glass.
- Stage IV: At pressures exceeding 55 GPa, impact melt rocks and glasses form by the complete melting of volcanic rocks.

Flows of impact melt on the crater walls were possibly the sources of these rocks before redeposition. Impact melt rocks are composed of dark glass matrix and numerous clasts of shocked rocks, minerals, and glasses. The fragments of impact glasses and shocked volcanic rocks have sharp contacts with the impact melt due to rapid cooling of the rocks. The composition of the impact melt rocks and melt breccias is similar to the composition of acid volcanic rocks found at the crater.

Impact glasses occur not only inside the crater but are also common on the outer slopes of the structure. The aerodynamical shape of glass bombs indicates their formation during transportation in the atmosphere. Ablation of some bomb surface is evidence for solidification and remelting while traveling on very steep trajectories. The composition of impact glasses is very similar to the composition of volcanic rocks of the upper, 250 m-thick, layer of the crater basement; the closest similarity is observed for ignimbrites.

Previous studies of siderophile element contents in impact melt rocks and impact melt glasses have shown only minor enrichment in Cr, Ni, and Co compared to target rocks; this was also confirmed in the present study for Ir, the maximum content of which was found to be on the order of 100 ppt. The most pronounced enrichment is for Cr, which could indicate an achondritic projectile. However, no unambiguous conclusions regarding the presence and nature of a meteoritic component in the El'gygytgyn impactites can be made so far.

Acknowledgments–We are grateful to Dr. E. Gurova for optical measurements of impact rocks and to R. Rakitskaya for X-ray diffraction analyses. This work was supported by the Austrian Science Foundation (project Y58-GEO, to C. Koeberl) and by the International Exchange Programs of the Austrian Academy of Science and the University of Vienna (to E. Gurov and C. Koeberl). We are grateful to P. Claeys, A. Deutsch, and R. Schmitt for detailed and helpful reviews of the manuscript.

Editorial Handling—Dr. Alexander Deutsch

REFERENCES

Brigham-Grette J., Glushkova O., Minyuk P., Melles M., Overdun P. P., Zielke A., Nowacyzk N., Nolan M., Stone D., and Layer P. 1998. Preliminary lake coring results from El'gygytgyn crater, eastern Siberia (abstract). *Eos Transactions, American Geophysical Union* 79:F477.

Chao E. T. C. 1963. The petrographic and chemical characteristics of tektites. In *Tektites,* edited by O'Keefe J. A. Chicago: University of Chicago Press. pp. 51–94.

Dabija A. I. and Feldman V. I. 1982. Geophysical characteristics of some astroblemes of USSR. *Meteoritika* 40:91–101. In Russian.

Dietz R. S. 1977. El'gygytgyn crater, Siberia: Probable source of Australasian tektite field (and bediasites from Popigai). *Meteoritics* 12:145–157.

Dietz R. S. and McHone J. F. 1976. El'gygytgyn: Probably world's largest meteorite crater. *Geology* 4:391–392.

Engelhardt W. V. 1972. Shock-produced rock glasses from the Ries crater. *Contributions to Mineralogy and Petrology* 36:265–292.

Engelhardt W. V. 1974. Meteoritenkrater. *Naturwissenschaften* 61: 413–422.

Feldman V. I., Granovsky L. B., Kapustkina I. G., Karoteeva N. N., Sazonova L. V., and Dabija A. I. 1981. Meteorite crater El'gygytgyn. In *Impactites,* edited by Marakhushev A. A. Moscow: Moscow State University Press. pp. 70–92. In Russian.

Gurov E. P. and Gurova E. P. 1979. Stages of shock metamorphism of volcanic rocks of acid composition on example of the El'gygytgyn crater (Chukotka). *Doklady Academii Nauk* 249: 1197–1201. In Russian.

Gurov E. P. and Gurova E. P. 1982. Composition of impact melt rocks of the El'gygytgyn crater and content of Ni and Cr in them. In *Kosmicheskoe veschtestvo na Zemle,* edited by Sobotovich E. V. Kiev: Naukova Dumka Press. pp. 120–123. In Russian.

Gurov E. P. and Gurova E. P. 1983. Regularities of fault spreading around meteorite craters (an example of the El'gygytgyn crater). *Doklady Academii Nauk* 275:958–961. In Russian.

Gurov E. P. and Gurova E. P. 1991. *Geological structure and rock composition of impact structures.* Kiev: Naukova Dumka Press. 160 p. In Russian.

Gurov E. P. and Yamnichenko A. Y. 1995. Morphology of rim of complex terrestrial craters (abstract). 26th Lunar and Planetary Science Conference. pp. 533–534.

Gurov E. P., Valter A. A., Gurova E. P., and Serebrennikov A. I. 1978. Impact meteorite crater El'gygytgyn in Chukotka. *Doklady Academii Nauk* 240:1407–1410. In Russian.

Gurov E. P., Gurova E. P., and Rakitskaya R. B. 1979a. Stishovite and coesite in shock-metamorphosed rocks of the El'gygytgyn crater in Chukotka. *Doklady Academii Nauk* 248:213–216. In Russian.

Gurov E. P., Valter A. A., Gurova E. P., and Kotlovskaya F. I. 1979b. El'gygytgyn impact crater, Chukotka: Shock metamorphism of volcanic rocks (abstract). 10th Lunar and Planetary Science Conference. pp. 479–481.

Hawke B. R. and Head J. W. 1977. Impact melt on lunar craters rims. In *Impact and explosion cratering,* edited by Roddy D. J., Pepin R. O., and Merrill R. B. New York: Pergamon Press. pp. 815–841.

Kapustkina I. G., Kolesov G. M., and Feldman V. I. 1985. Contamination of the El'gygytgyn crater impactites with meteoritic matter. *Doklady Academii Nauk* 280:755–758. In Russian.

Koeberl C. 1990. The geochemistry of tektites: An overview. *Tectonophysics* 171:405–422.

Koeberl C. 1993. Instrumental neutron activation analysis of geochemical and cosmochemical samples: A fast and reliable method for small sample analysis. *Journal of Radioanalytical and Nuclear Chemistry* 168:47–60.

Koeberl C. and Huber H. 2000. Optimization of the multiparameter γ-γ coincidence spectrometry for the determination of iridium in geological materials. *Journal of Radioanalytical and Nuclear Chemistry* 244:655–660.

Komarov A. N., Koltsova T. V., Gurova E. P., and Gurov E. P. 1983. Determination of the El'gygytgyn crater impactites' age by the fission track method. *Doklady Academii Nauk* 10:11–13. In Russian.

Kotlar I. N., Beliy V. F., and Milov A. P. 1981. *Petrochemistry of magmatic formations of the Ochotsk-Chukotsk volcanogenic belt.* Moscow: Nauka Press. 221 p. In Russian.

Layer P. W. 2000. Argon-40/argon-39 age of the El'gygytgyn event, Chukotka, Russia. *Meteoritics & Planetary Science* 35:591–599.

Nekrasov I. A. and Raudonis P. A. 1963. Meteorite craters. *Priroda* 1:102–104. In Russian.

Nolan M., Liston G., Prokein P., Brigham-Grette J., Sharpton V. L., and Huntzinger R. 2003. Analysis of lake ice dynamics and morphology on Lake El'gygytgyn, NE Siberia, using synthetic aperture radar (SAR) and Landsat. *Journal of Geophysical Research* 108:3-1–3-12, doi: 10.1029/2001JD000934.

Nowaczyk N. R., Minyuk P., Melles M., Brigham-Grette J., Glushkova O., Nolan M., Lozhkin A. V., Stetsenko T. V., Andersen P. M., and Forman S. L. 2002. Magnetostratigraphic results from impact crater Lake El'gygytgyn, northeastern Siberia: A 300 kyr long high-resolution terrestrial palaeoclimatic record from the Arctic. *Geophysical Journal International* 150: 109–126.

Obruchev S. V. 1957. *Across the tundra and mountains of Chukotka.* Moscow: State Press of Geography. 198 p. In Russian.

O'Keefe J. A. 1976. *Tektites and their origin.* Amsterdam: Elsevier. 254 p.

Reimold W. U., Koeberl C., and Bishop J. 1994. Roter Kamm impact crater, Namibia: Geochemistry of basement rocks and breccias. *Geochimica et Cosmochimica Acta* 58:2689–2710.

Stähle V. 1972. Impact glasses from the suevites of the Nördlinger Ries. *Earth and Planetary Science Letters* 17:275–293.

Stöffler D. 1971. Progressive metamorphism and classification of shocked and brecciated crystalline rocks. *Journal of Geophysical Research* 76:5541–5551.

Stöffler D. 1974. Deformation and transformation of rock-forming minerals by natural and experimental shock processes: II. Physical properties of shocked minerals. *Fortschritte der Mineralogie* 51:256–289.

Stöffler D. and Langenhorst F. 1994. Shock metamorphism of quartz in nature and experiment: I. Basic observations and theory. *Meteoritics* 29:155–181.

Storzer D. and Wagner G. A. 1979. Fission track dating of El'gygytgyn, Popigai, and Zhamanshin craters: No source for Australasian or North American tektites (abstract). *Meteoritics* 14:541–542.

Taylor S. R. and McLennan S. M. 1985. *The continental crust: Its composition and evolution.* Oxford: Blackwell Scientific Publications. 312 p.

Zotkin I. T. and Tsvetkov V. I. 1970. Search of meteorite craters on the Earth. *Astronomitcheskiy Vestnik* 4:55–65. In Russian.